

Broadband Excitation of ECR Plasmas*

Wayne D. Cornelius, Scientific Solutions, San Diego CA USA †

D. Leitner, M. Galloway, Lawrence Berkeley National Laboratory, Berkeley CA, USA

D. P. May, Cyclotron Institute, Texas A&M University, College Station, Texas USA

R. D. Penny, SAIC, San Diego CA USA

Abstract

Scientific Solutions developed an rf source capable of producing a variety of rf spectra for excitation of ECR plasmas at 2.45, 6.5, 14.5, 18.0 and 28.0 GHz. This device replaces the crystal oscillator in the rf chain and is essentially a software-defined radio transmitter that allows the user to select from a variety of different rf spectral patterns via an Ethernet link. Two specific patterns were chosen for our initial series of tests: 1) a simultaneous multimode pattern comprised of n rf-modes within a specified bandwidth and 2) a chirp spectral pattern comprised of n discrete frequencies where the chirp bandwidth, slew direction, and slew rate are user-selectable. In either case n is a user-defined value between 1 and 1024. This paper describes the design of the rf circuit and its theory of operation. Initial results of our tests with the 6.4 and 14.5 GHz ECR sources at Texas A&M University and with the AECR-U at the Lawrence Berkeley National Laboratory are also presented.

BACKGROUND

ECR sources depend on coupling energy into plasma electrons via the electron-cyclotron resonance. Plasma electrons transiting the resonance region inside the source absorb energy from the radio-frequency field. The change in electron energy is determined by the magnitude of the rf field in the resonance zone integrated over the time required to transit the zone. The effective width of the resonance zone is derived from the gradient of the magnetic field (dB/dz) and the bandwidth of the rf energy. Therefore to increase the volume of the resonance zone, we need to decrease the field gradient or increase the rf bandwidth. The question addressed here is: given a constant field gradient, which is more efficient in transferring rf energy to plasma electrons: 1) high peak rf power with a narrow resonance zone, or 2) lower peak power with a wider zone?

Kawai et. al. reported on experiments using an rf noise source to increase the rf bandwidth.[1] These experiments showed marginal improvement of ion current in a plateau style ECR source, but did show enhanced operational stability compared with single-frequency excitation. More recent experiments with a minimum-B configuration ECR source [2] demonstrated significant

benefits of broadband excitation in producing Ar^{11+} ions with 400 W of rf power.

A possible reason for the lack of improved ion current in the first case is that noise sources have no coherence between adjacent frequency bins. Therefore an electron transiting one frequency bin has a 50% probability of encountering the opposite phase in the adjacent bin, thereby decelerating the electron instead of continuing to accelerate it. Generating an rf spectrum in a coherent manner populates adjacent frequency bins with phase-related rf energy. Hence a modulated rf source may provide just the coherence needed to improve the rf coupling efficiency. The trick lies in discovering the optimal modulation scheme(s).

RF MODULATOR AND KLYSTRON DRIVER CIRCUIT

To investigate broadband radio frequency (rf) excitation of ECR plasmas, we utilized a software-defined radio transmitter (RF Injection Device or RID) originally developed for another application. This device, created to automatically analyze resonant frequency spectra between 100 MHz and 1 GHz, was modified to produce a variety of user-selectable spectra in the 1-2 GHz band. The baseband rf signal from the modified RID is passed through an Analog Devices AD8349 quadrature modulator that provides complete control of the rf waveform within a 20 MHz bandwidth centered around the operating frequency. The output waveform of the AD8349 is frequency multiplied into the range of interest using a variety of multiplier chains and amplifier circuits as illustrated in figure 1. The exact configuration of the multiplier chain depends on the target frequency range. The AD8349 actually supports much wider bandwidth. However we restricted the baseband frequency range to 20 MHz in order to keep the frequency-multiplied bandwidth within a reasonable range so as not to stress the klystron amplifiers typically used for ECR heating.

The operation of the RID is controlled by an embedded Xilinx processor connected via Ethernet to the user's computer running the interface control panel. Because the frequency synthesis is under complete software control, we can easily adjust the operating frequency, the bandwidth, and fill factor (i.e. the mode spacing) up to the limits of the AD8349.

As shown in figure 1, the output spectrum of the RID is frequency multiplied in a variety of circuits whose configuration depends on the desired operating frequency (figure 1). Note that the operating bandwidth of the overall chain is multiplied by the same factor--multiplying

*This material is based upon work supported by the U.S. Department of Energy under Award Number DE-FG02-04ER84166. The views and opinions of authors expressed herein do not necessarily state or reflect those of the United States Government or any agency thereof.

†Current address: SAIC, 10740 Thornmint Road, San Diego CA 92127

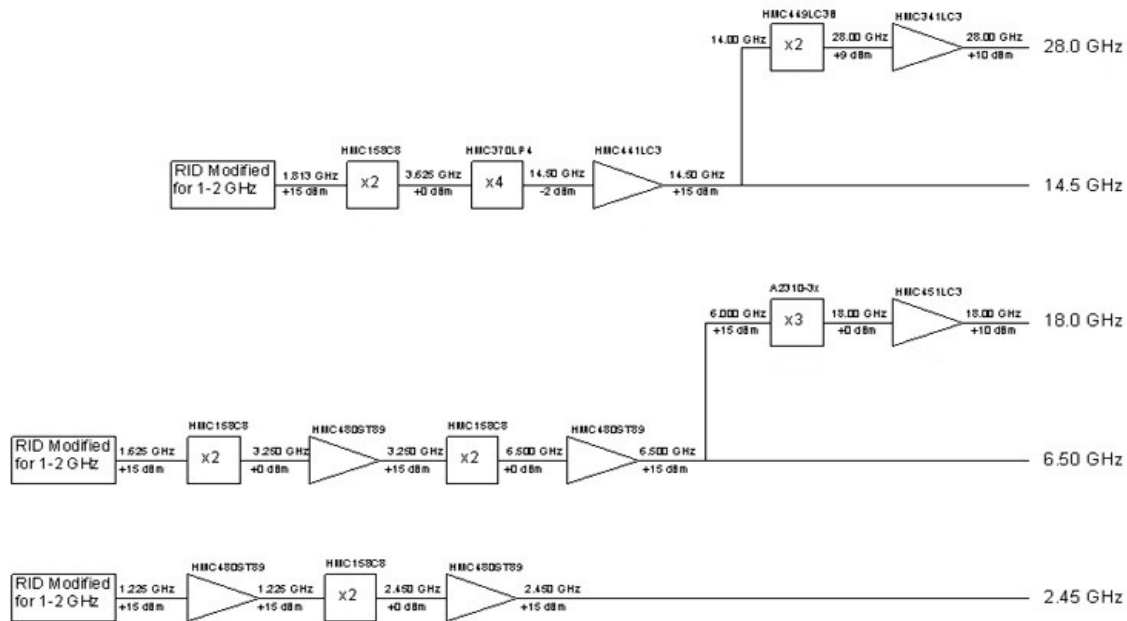


Figure 1. Detail of the frequency multiplier chains for common ECR frequency bands.

the frequency by a factor of four increases the bandwidth by a factor of four. A complication of this approach is that the anti-aliasing filters used to eliminate spurious frequencies (spurs) in the baseband cannot eliminate spurs resulting from the multiplication process. The effect of these spurs is to produce mirror images of the mode structure around the center frequency. In general these additional spurs are mostly annoying. The primary effect is a larger number of frequencies in the rf spectrum than the software setpoint. These spurs would be a major problem in rf communications systems, but are not a significant problem in rf heating applications.

Figure 2 shows how two frequency-doubling processes transform a single-frequency spectrum at 1.60 GHz into a 9-mode structure at 6.40 GHz. Although the mode structure of figure 2 looks daunting on the semi-log scale, the power in these spurious modes is less than 1% of the total. These spurious frequencies would pose significant problems in rf communications systems, but are not a significant problem in the plasma-heating process.

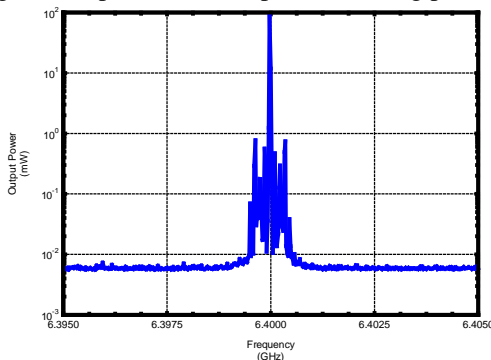


Figure 2. Single-mode power spectrum following frequency quadrupling from 1.6 to 6.4 GHz.

RF Comb Spectrum

The embedded Xilinx code utilizes a phase-hopping scheme and/or a frequency chirp to generate the frequency spectra. The series of phase changes in a single-frequency rf transmission are Fourier transformed into a frequency comb spectrum. The relative power in each tooth of the comb is a function of the phase-hopping pattern. A power spectrum with relatively uniform power in each mode is produced by visiting each possible phase change once during the transmit cycle. In other words, the phase diagram is divided into n segments (n is the number of modes in the spectrum so the 2π phase sheet is divided into n segments of $\Delta\phi$ phase width). The phase of the transmitted rf is sequentially stepped by values that visits all possible phase differences (i.e. $1x, 2x, 3x, \dots, n\Delta\phi$). The number of modes (up to 1024) and the initial phase offset are under user-control. The relative power in each mode depends on the particular sequence of phase changes in the algorithm. Figure 3 compares the mode structure for a variety of different mode-hopping settings (1, 3, 4, 8, 16, 32, and 64 modes). The red curves denote the power in dB and the blue curves show the power on a linear scale.

RF Chirp Spectrum

Alternatively we can generate a chirp spectrum by slewing the frequency either up or down using n -steps within a specified bandwidth ($n=1024$). The bandwidth and the dwell-time on each frequency step are under user control.

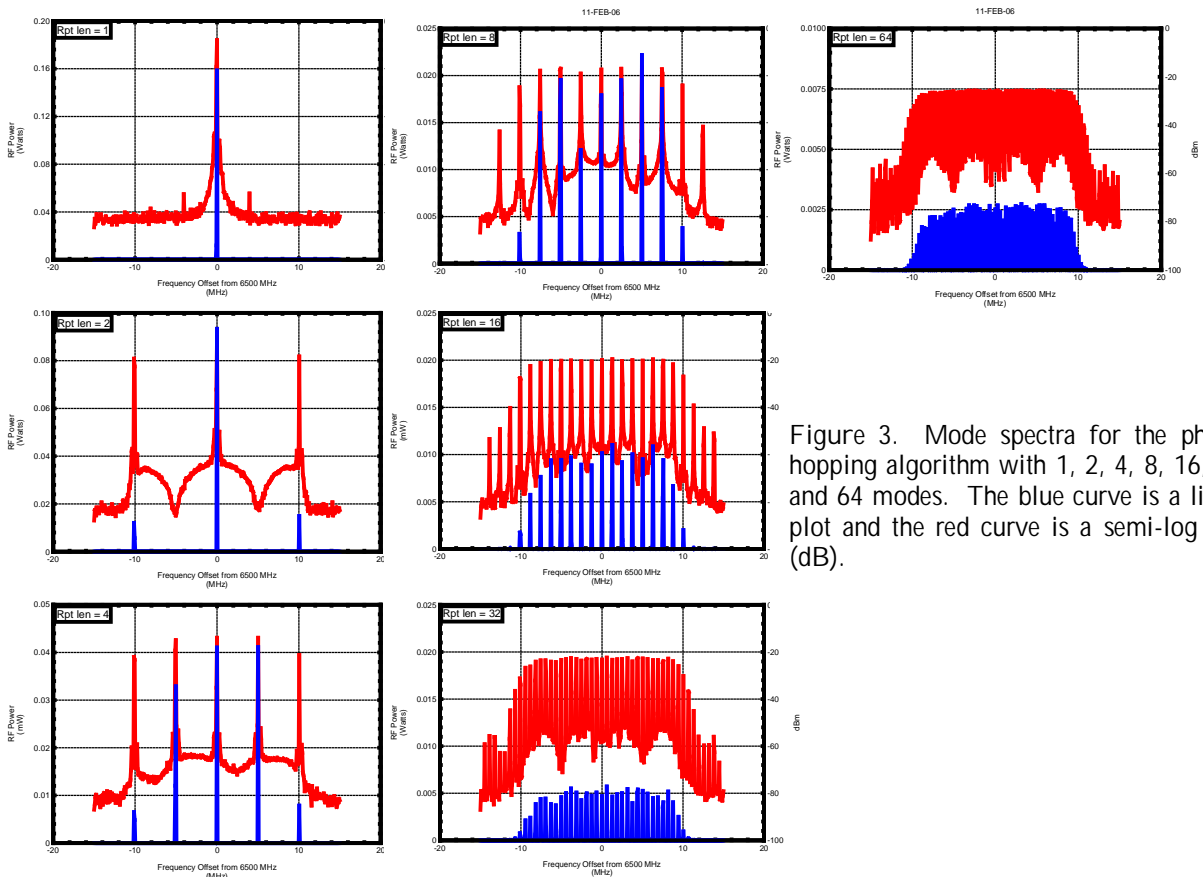


Figure 3. Mode spectra for the phase-hopping algorithm with 1, 2, 4, 8, 16, 32, and 64 modes. The blue curve is a linear plot and the red curve is a semi-log plot (dB).

Displays of chirp-mode spectra can be less revealing than comb-spectrum displays because an accurate representation of the spectrum is produced only when the scan rate is very slow compared with the slew rate of the chirp. Figure 4 (figure 5) compares rf excitation spectra (semi-log plots) for 1-, 2-, and 3-mode excitation at 6.4 GHz with $TSRPT = 1(10)$. The Time-Slice Repeat (TSRPT) value sets the number of clock cycles the chirp remains in each frequency bin before moving on to the next bin. Note how increasing TSRPT reduces the power-weighted bandwidth of the excitation spectrum because the frequency remains for a longer duration at each frequency step. As we noted above, phase changes generate the frequency sidebands. Therefore dwelling for a longer period of time on each frequency reduces the number of phase changes per unit time and hence the number of spurious frequencies in the sidebands.

Figure 6 compares chirp spectra with 1, 2, 3, and 16 modes in a 4.3 MHz bandwidth centered around 6.40 GHz (semilog plot). Note how the number of modes and their separation within the peak of the spectrum coalesces into a solid bandwidth of frequencies. Figure 7 shows how the spurious frequencies disappear as the dwell time on each frequency increases.

RF COMBINATION MODE SPECTRUM

The user can also choose to chirp a comb spectrum. The frequency agility and flexibility allowed by these two modulation schemes provides a means for testing the efficacy of broadband excitation of the ECR plasmas under a wide variety of circumstances.

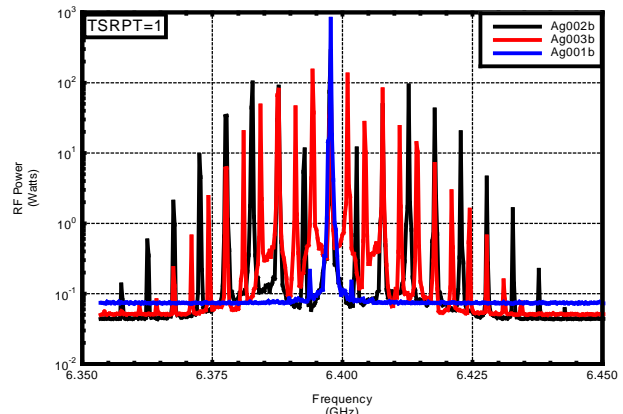


Figure 4. Comparison of rf excitation spectra with $TSRPT=1$ (1 mode=blue, 2 modes=black, 3 modes=red).

TEST RESULTS

A series of experiments were performed with the 6.4 GHz and 14.5 GHz ECR sources at Texas A&M University and with the 14.5 GHz AECR-U source at LBNL. Results of these tests are described below. Although the results of these tests did not show a dramatic improvement in ion current, some very interesting features were discovered that warrant further experimentation. These features include 1) improved plasma stability when operating with a multimode rf spectrum, 2) significantly improved operation for oxygen beams when operating at lower rf power levels, 3) slight improvement in ion currents for the highest measurable charge states, and 4) the opportunity to tune the frequency to better couple the rf power into the ion source.

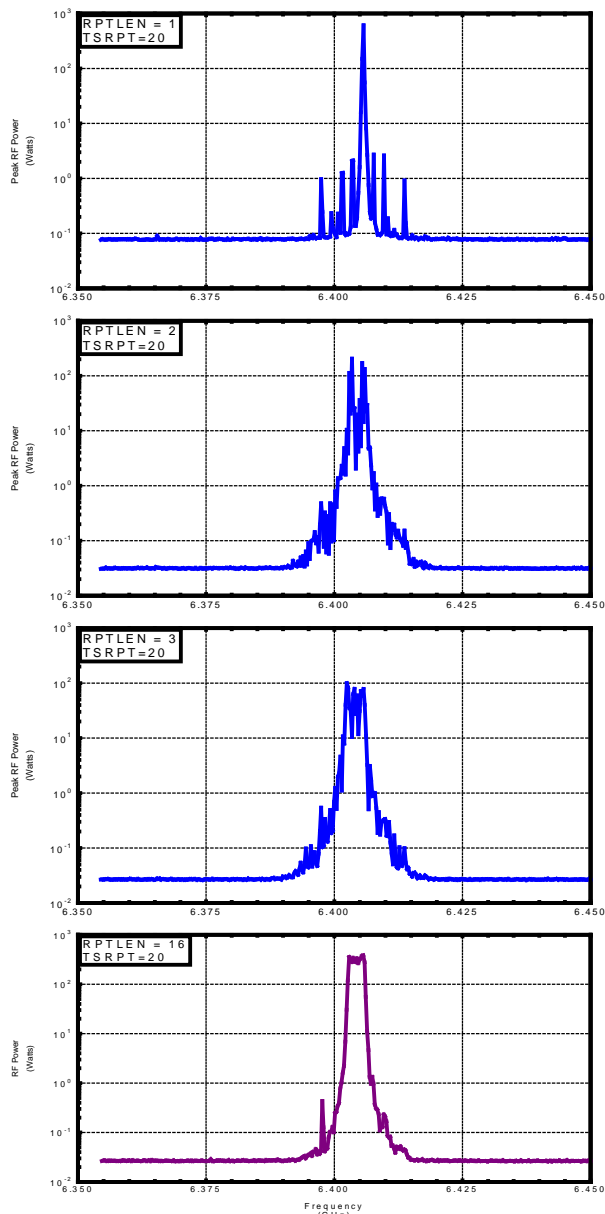


Figure 5. Comparison of rf excitation spectra with TSPRT=10 (1 mode=blue, 2 modes=red, 3 modes=black).

RESULTS FROM TAMU: COMB SPECTRUM EXCITATION

Figure 8 compares the O^{7+} ion current extracted from the TAMU 14.5 GHz ECR source as a function of rf power. The blue curve shows the ion current produced with a single mode in the rf spectrum whereas the red curve shows the ion current produced with two rf modes in the excitation spectrum. Although the two curves in figure 4 converge at higher power levels, at a power level of 500 Watts, multimode operation produced nearly 40% more ion current than single-mode excitation. This result correlates well with the results of Kawai et. al. [2] and Celona, et. al. [3]

Figure 9 summarizes results with 1-, 2-, and 3-mode excitation of the plasma in producing a Au^{23+} beam with the 6.4 GHz source. This particular ion is highly charged

and requires high rf power levels. Unlike the O^{7+} results, we observed no benefit with multimode excitation at the lower rf power levels. However some slight benefit can be seen for 2- and 3-mode excitation at the highest power levels. Note also that rf spectra with an odd-number of modes seemed to have slightly greater efficiency than spectra with even numbers of modes. Perhaps this effect is because the odd-number excitation always has a mode in the center of the band whereas the even number has a gap between rf modes in the center of the band. This odd-even effect is only evident with relatively few rf modes in the spectrum (e.g. 7-mode excitation has a performance equivalent to 8-modes whereas 3-modes seem to have an advantage over 2-mode excitation).

Figure 10 compares 1-mode and 3-mode rf excitation in producing an Ar^{12+} beam with the 14.5 GHz source at TAMU. Note how the ion source changed plasma modes around 900 watts of excitation. As was the case for the oxygen beam, multimode excitation appears to improve the ion current at intermediate power levels, but this difference disappears at the highest power levels. The two 3-mode data points surrounding the 1-mode value at 1050 watts suggests that fine-tuning the ion source could recover the missing 3-mode ion current compared with the 1-mode value.

Figure 11 shows the Kr^{19+} ion current as a function of rf power and the number of excitation modes. This figure shows a clear benefit of multimode excitation compared with single-mode excitation. The 2-mode and 3-mode spectra produced a 6% increase in Kr^{19+} current and an 11% increase in Kr^{20+} current with 1.28 kW of rf power.

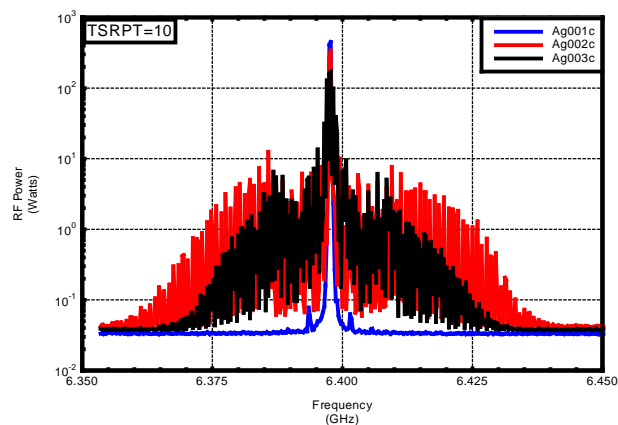


Figure 6. Chirp spectra with 1-, 2-, 3-, and 16-modes in a 4.3 MHz bandwidth (semi-log plots).

RESULTS FROM TAMU: CHIRP SPECTRUM EXCITATION

Figure 6 showed chirp spectra with 1-, 2-, 3-, and 16-modes in a 4.3 MHz bandwidth at 6.40 GHz. These spectra resulted in 1.36, 1.45, 1.49, and 1.50 μA respectively of Ag^{25+} beam ions with 0.9 kW of rf power and a 1 usec dwell time at each frequency. Figure 12 compares the performance of a 1-mode chirp with a 16-mode chirp with a Ag^{25+} beam as a function of rf power.

This figure shows some improvement in performance for a 16-mode chirp at nearly all rf power levels.

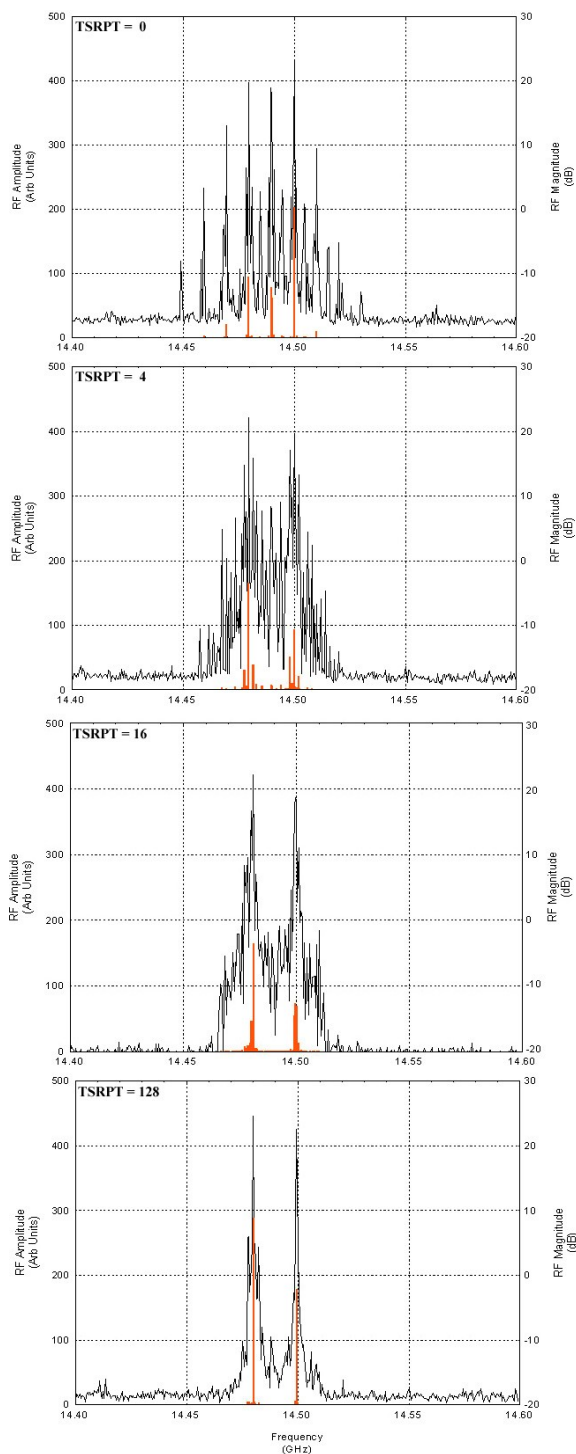


Figure 7. Chirp spectra with TSRPT = 0, 4, 16, and 128 (black: linear scale, red: semi-log scale).

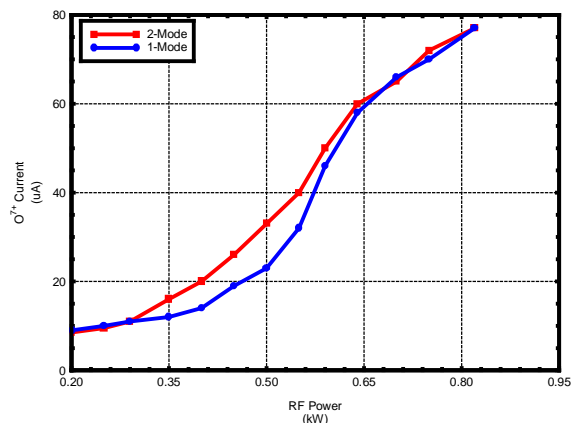


Figure 8. Oxygen 7+ current extracted from the TAMU 14.5 GHz ECR source as a function of rf power level for single-mode (blue curve) and two-modes (red curve) in the rf spectrum.

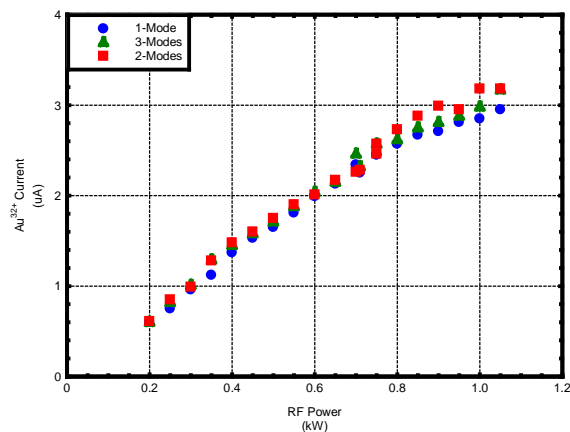


Figure 9. Plot of Au^{32+} current as a function of rf power and the number of rf excitation modes.

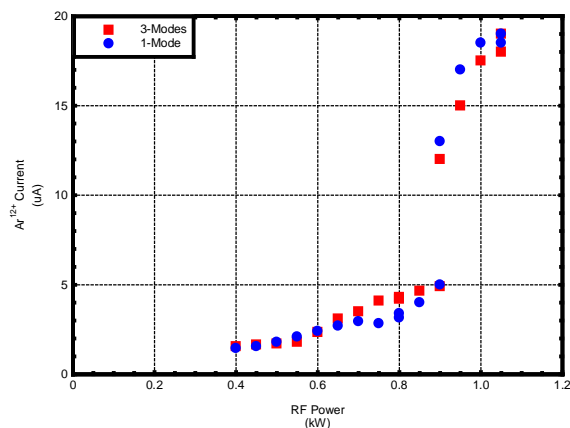


Figure 10. Plot of Ar^{12+} current as a function of rf power and the number of rf excitation modes at 6.4 GHz.

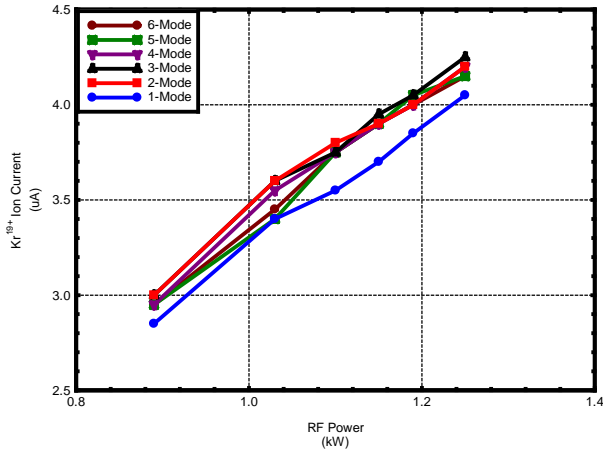


Figure 11. Plot of Kr^{19+} current as a function of rf power and the number of excitation modes at 14.5 GHz.

In summary, the data obtained with the TAMU 6.4 and 14.5 GHz ECR sources are encouraging in that some performance improvement was obtained for broadband excitation compared with single-mode excitation of the plasma. However the magnitude of this improvement is relatively modest, generally being less than 10% for the higher charge states and heavier ion species. This noted however, we observed substantial improvement in broadband performance at the lower power levels for O^{7+} in figure 4. We also noted significant improvement in the Ag^{25+} current in figure 12, particularly at the lower rf power levels. These observations correlate well with results reported in reference 3.

During experiments at LBNL (discussed in the next section), we discovered that some of the ion current lost in switching to broadband excitation could be recovered by retuning the ion source. The experimental procedure at TAMU was to optimally tune the ion source with single-mode excitation and then change the rf spectrum using software commands. In most, if not all, cases, multimode rf excitation improved the performance, but no significant retuning of the ion source was attempted. It is also important to note that the base vacuum pressure of the TAMU 6.4 GHz source was approximately a factor of two higher than the optimal pressure. How much of an effect this higher pressure had on these experiments is unclear. This increased base pressure may have masked performance changes that might have been obtained by retuning the TAMU source (as was observed with the AECR-U source). The excellent base vacuum pressure in the AECR-U source may have reduced the sensitivity to differences in single- versus multi-mode rf excitation.

RESULTS FROM LBNL: COMB SPECTRUM EXCITATION

Figure 13 compares the O^{5+} , O^{6+} , and O^{7+} ion currents extracted from the LBNL AECR-U source operating at 14.30 GHz. Unlike the data in Figure 4, each data point in this figure represents the optimal tuning of the ion source at each rf setting. The ion currents obtained with single-mode rf excitation are denoted by the solid-curves

and the currents obtained with two-mode rf excitation are denoted by the dashed curves. In both figure 13 and in figure 8, the ionization appears to saturate at higher rf power levels so that no difference is observed between single- and multi-mode rf excitation patterns at the highest power levels. Note however that multi-mode excitation significantly increases the ion current for rf power levels between 500 and 600 Watts – particularly for the 6^+ and 7^+ charge states.

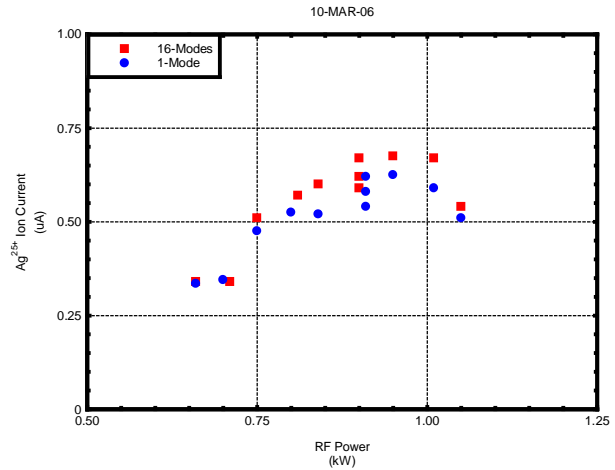


Figure 12. Comparison of Ag^{25+} ion current produced with the 1- and 16-mode chirp spectra from figure 8 as a function of rf power.

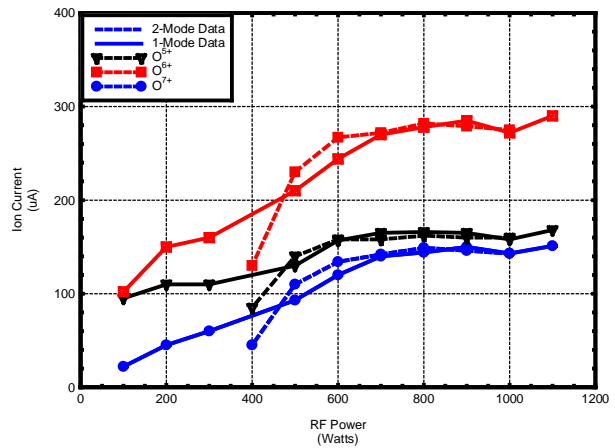


Figure 13. Oxygen 5^+ (black), 6^+ (red), and 7^+ (blue) ion currents extracted from the LBNL AECR-U ECR source as a function of rf power level for single-mode (solid curves, open symbols) and two-modes (dashed curves, closed symbols) in the rf spectrum. Each data point represents the optimized ion current for each rf setting.

Figure 14 shows the rf power spectrum of the AECR-U klystron amplifier for single-mode excitation. Unfortunately the GPIB cable was not available during the test program at LBNL so the rf spectra were captured from the spectrum analyzer display with a digital camera. As a result, these spectral data can be displayed, but cannot be analyzed (as was possible with the TAMU data). Figure 15 (16) shows a linear (semi-log) plot of the rf power spectrum for multimode rf excitation.

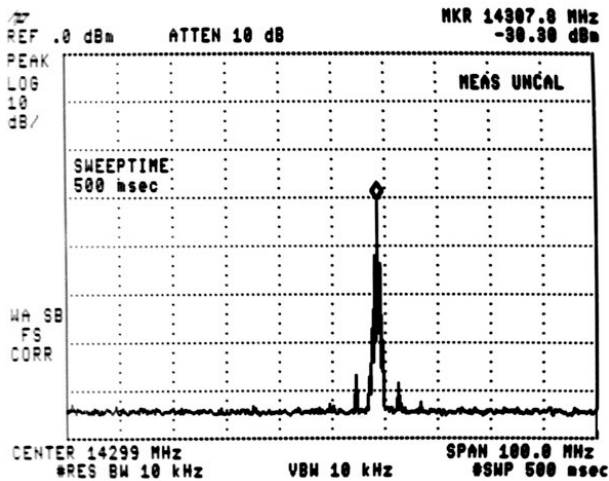


Figure 14. Single-mode rf spectrum at the output of the AECR-U klystron amplifier (dB scale).

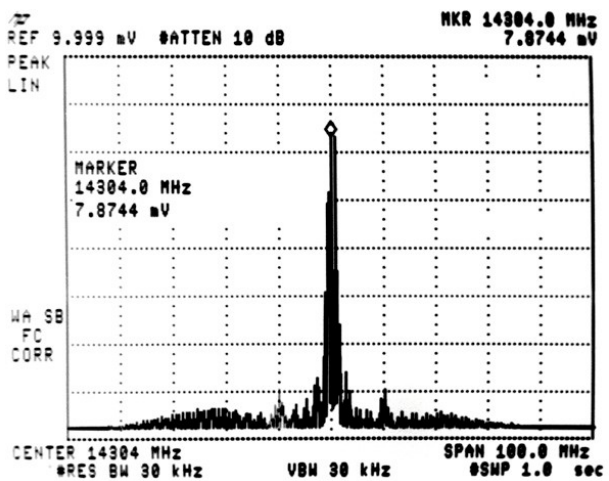


Figure 15. Multi-mode rf spectrum of the AECR-U klystron (linear scale). Note the significant satellite frequency bands on both sides of the central peaks.

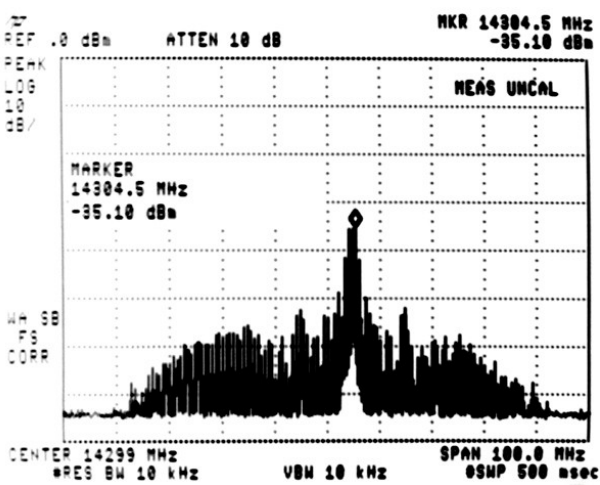


Figure 16. Multi-mode rf spectrum of the AECR-U klystron (semi-log plot).

Figure 17 shows the reflected power spectrum from the AECR-U source. Note how the lower sideband has significantly lower reflected power than the upper sideband. This effect was a clue that the operating frequency of the AECR-U source was set too high for optimal operation.

Figures 18 and 19 compare the forward and reflected power spectra for the AECR-U source operating with Xenon gas and 1024 modes in a 100 MHz chirp spectrum. The forward power is relatively uniform with frequency whereas the reflected power shows power absorption only from the center 30 MHz. At the conclusion of these experiments, the crystal oscillator rf source for the AECR-U was retuned approximately 30 MHz lower in frequency so that the operating frequency was closer to the frequency with minimum reflected power.

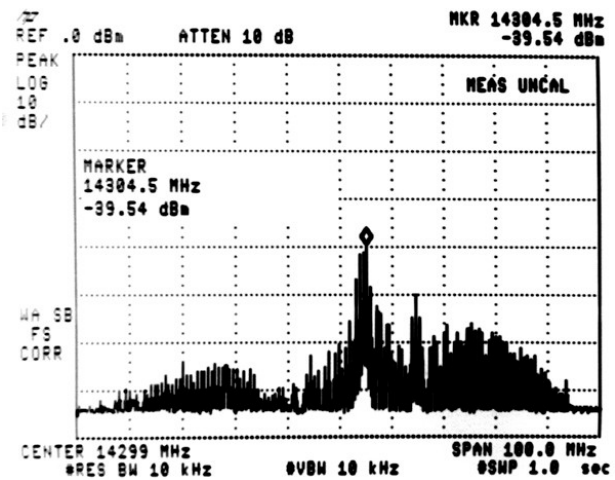


Figure 17. Reflected rf power spectrum corresponding to the multi-mode transmitted rf spectrum of figure 15 (semi-log plot). Note how the plasma absorbed more power from the lower frequency satellite band than from the upper satellite band.

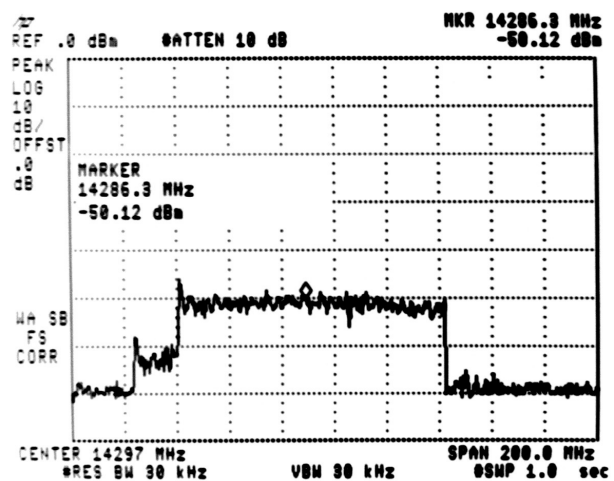


Figure 18. Forward power spectrum from the AECR-U source operating with Xe gas (linear scale). The klystron was producing a flat power spectrum with 1024 modes in a 100 MHz bandwidth.

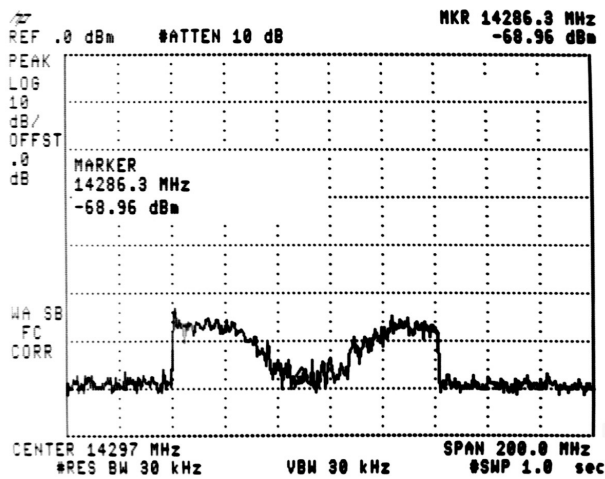


Figure 19. Reflected power spectrum from the AECR-U source operating with Xe gas (linear scale). The plasma was absorbing power from only the central 30 MHz of the spectrum shown in figure 18.

Figure 20 shows a ^{209}Bi spectrum for two-frequency rf heating. LBNL pioneered the techniques for two-frequency excitation of ECR plasmas. They employed rf power at 14.3 and 10 GHz to form two ECR regions in the plasma. This approach demonstrated significant improvement over single-frequency sources. One of the goals of our research project was to determine if multiple frequency heating would prove advantageous when the separation between the two frequencies was relatively small. As noted in the TAMU experiments, in-band 2-mode heating showed some improvement, but not as much as the K- and X-band heating approach used by LBNL. Note however that the 32-mode chirp spectrum improved the charge-state distribution as evidenced by a reduction of ion current at the lower charge-states (21^+ , 22^+ , and 25^+) with an accompanying increase in ion current at the highest charge-states (31^+ through 37^+). While relatively modest gains in charge-state distributions were observed, the 32-mode chirp resulted in more stable operation of the AECR-U.

Figure 21 is a comparison of various multi-mode chirp spectra along with single-mode heating for ^{209}Bi using two-frequency heating (14.3 and 10 GHz). Each of the traces in this figure represents the optimal performance achieved by fine-tuning the source parameters. Figure 22 is a close-up of the region detailing the highest charge states. The slight advantage of multimode heating is shown by the general shift of the red curve to higher values at higher charge states and lower values at lower charge states. Note that multi-mode excitation was always equal to or better than single-mode excitation. Figure 23 details the charge-state distribution for the highest measurable charge states in ^{209}Bi with dual-frequency heating (multi-mode at 14.3 GHz and single mode at 10 GHz). This figure shows the slight improvement in current for all charge states with multi-mode rf at 14.3 GHz. Figure 24 details the ^{129}Xe charge-

state distributions for a variety of chirp spectra at 14.3 GHz. Note that the 32-mode chirp spectrum shows significant improvement compared with single-mode excitation.

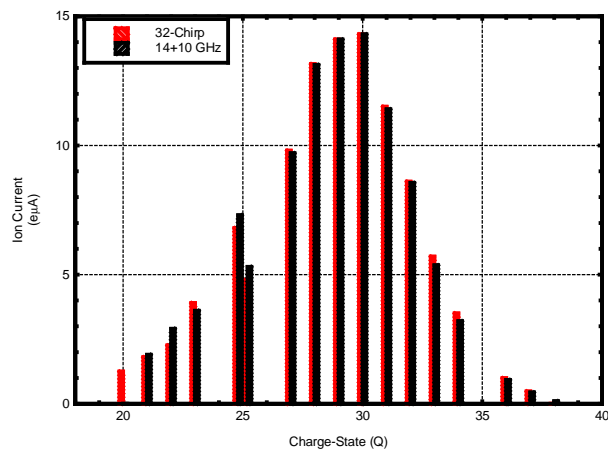


Figure 20. Charge-state distribution of ^{209}Bi Beam with 2-frequency heating. The values from normal AECR two-frequency heating (single-mode 10 and 14.3 GHz) is given by the black bars whereas the red bars indicate the current obtained with a 32-mode, 13.3 MHz chirp at 14.3 GHz in combination with the 10 GHz single-mode rf power.

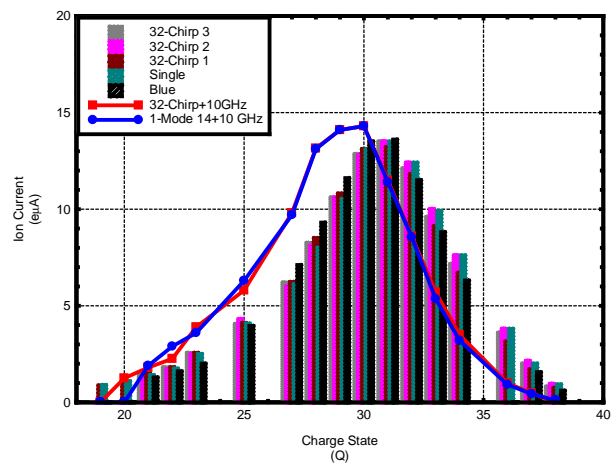


Figure 21. Charge-state distribution of ^{209}Bi Beam with multi-mode chirp at 14.3 GHz and 2-frequency heating (14.3 and 10 GHz).

CONCLUSION

The test results described above are interesting but not conclusive. Multi-mode rf heating showed some improvement compared with single-mode heating under most circumstances. However the improvement was generally modest (*5-10%) at the highest power levels and for the highest measurable charge states. Significant improvement was noted at lower rf power levels in some of the experiments, but this difference decreased with increasing rf power. The test program at LBNL demonstrated significant improvement in operational stability with multimode excitation. While it was usually possible to retune the AECR-U to achieve an equivalent

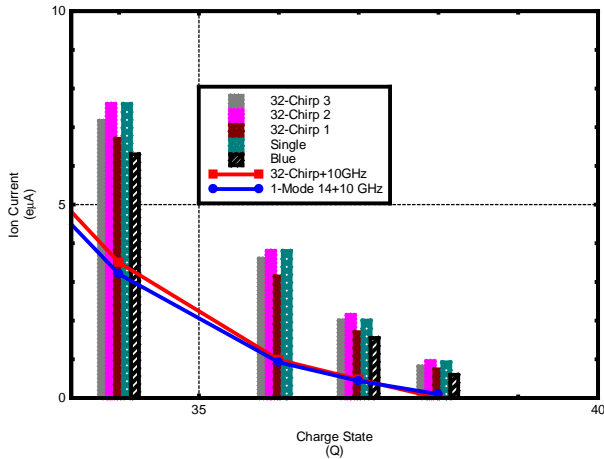


Figure 22. Close-up of the results at the highest charge-states shown in figure 21.

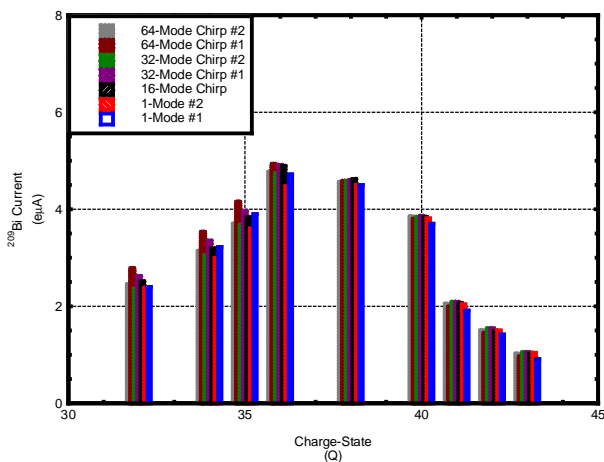


Figure 23. Charge-state distribution of ^{209}Bi Beam with multi-mode chirp at 14.3 GHz and 2-frequency heating. This figure details the region containing the highest measurable charge-states. Note the slight improvement obtained with a multi-mode chirp.

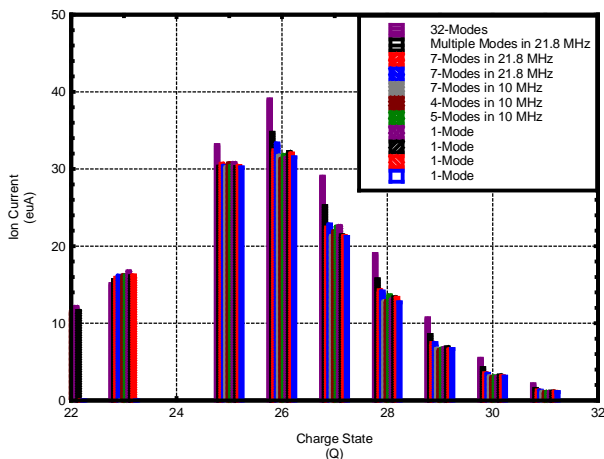


Figure 24. Charge-state distributions for Xe ions for a variety of rf excitation spectra. Note the significant improvement in performance provided by the 32-mode chirp compared with the single-mode results.

level of performance with single-mode excitation, the plasma was less stable with single-mode heating, often for periods exceeding several hours. Several times the AECR-U source was left operating with multi-mode rf for some period of time before it could be reliably switched over to single-mode rf heating. It is important to note that the AECR-U has a larger number of tuning knobs than are typical of ECR sources. It may not always be possible to achieve equivalent multi-mode and single-mode performance in ECR sources with fewer available tuning parameters.

The conclusion of these tests is that we do not yet have enough information on the efficacy of multi-mode heating. We observed modest improvement in charge-state distributions under some circumstances, but saw little effect under other conditions. The most significant observations are 1) the significant improvement in ion current when operating at less than optimal power levels, 2) the slight improvement in the ion currents of the highest charge-states, and 3) the improved operational stability. The improved stability might be significant enough to warrant switching to multi-mode heating under some conditions. The improvement in ion currents for the highest charge-states, while generally modest, might be enough to enable experimentation using those beams. Clearly more testing is needed.

REFERENCES

- [1] Y. Kawai, G.D. Alton, and Y. Lui, Proceedings of the 2005 Particle Accelerator Conference, Knoxville TN, p 1529
- [2] Y. Kawai, G. D. Alton, O. Tarmainen, P. Suominen, and H. Koivisto, Physics Letters A371(2007), p 307
- [3] L. Celona, S. Gammino, G. Ciavola, F. Consoli, and A. Galata, in Proc. 16th International Workshop on ECR Ion Sources, Berkely CA, AIP Conference Proceedings V749(2005) p.99